

## Electrochemical Detection of Arsenic in Various Water Samples

Muniyandi Rajkumar, Soundappan Thiagarajan, Shen-Ming Chen\*

Electroanalysis and Bio electrochemistry Laboratory, Department of Chemical Engineering and Biotechnology, National Taipei University of Technology, No.1, Section 3, Chung-Hsiao East Road, Taipei 106, Taiwan (ROC).

\*E-mail: [smchen78@ms15.hinet.net](mailto:smchen78@ms15.hinet.net)

Received: 10 June 2011 / Accepted: 17 July 2011 / Published: 1 August 2011

---

Nano Au-crystal violet (CRV) film has been fabricated on glassy carbon electrode (GCE) and indium tin oxide glass electrode (ITO) using cyclic voltammetry. The nano Au-CRV film modified GCE has been successfully employed for the detection of arsenic in lab and real drinking water sources like mineral water, spring water and tap water samples. The Nano Au-CRV film modified GCE successfully detects the arsenic in the linear range of 4 - 40  $\mu\text{M}$  with the detection limit of 0.20  $\mu\text{M}$  in lab samples. The proposed film successfully detects the arsenic in the commercial drinking water sources with sufficient detection limits.

---

**Keywords:** Crystal violet, gold nanoparticles, cyclic voltammetry, arsenic, differential pulse voltammetry.

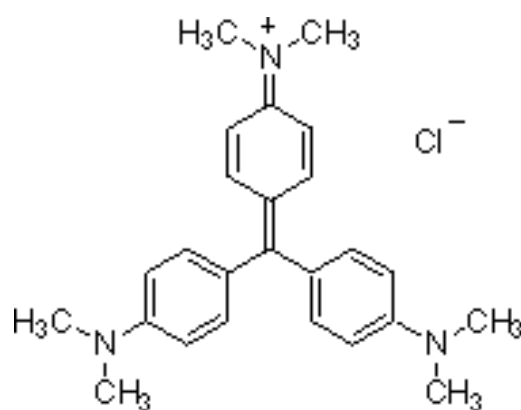
### 1. INTRODUCTION

Arsenic and its compounds were known as poisonous substances and widely distributed in the earth crust. In the ground water, arsenic exists in many chemical forms such as arsenite and arsenate and its direct exposure is toxic to humans, animals and the entire ecosystem [1, 2]. Arsenic compounds contamination is directly associated with cancer in lungs, skin, and bladder and kidney diseases. India, China, Bangladesh, Mexico, Argentina, USA and many other countries in the world reported the arsenic contamination in the ground water [3]. According to the world health organizations (WHO) report [4], the maximum permissible contamination of arsenic in the drinking water level is 10 ppb.

Hence there is a need for a sensitive and reliable method for detection of arsenic. Analytical methods, such as atomic absorption spectrometry, atomic fluorescence spectrometry and inductively coupled plasma with mass spectrometry have been used for the accurate detection of arsenic at the laboratory levels [5-8]. Along with these analytical techniques, electrochemical methods also found to

be convenient, reliable and important for the arsenic detection process [9-12]. For example, inorganic arsenic species have been detected in the sea water using a stripping chronopotentiometric (SCP) method [13]. In virtue of the electrochemical deposition, we can realize the successful determination of arsenic with a low detection limit, but it suffers from the interference by various metals like Cu, especially when it presents in a large amount in water systems. Copper can be easily co-deposited with the arsenic at the certain potential. Presence of copper can easily reduce the signal of the arsenic [14-16].

Crystal violet (CRV) is a well known organic dye used as an enhancer for bloody finger prints. The electrochemical properties of crystal violet have been described in various literature reports. CRVs applications in sensitized organic dye film [17], in the form of supporting electrolyte at liquid/liquid interfaces [18] and as dye chromophore [19] were reported.



Crystal Violet

Further, Dakkouri et al [20] and Haiss et al [21] showed that crystal violet had changed the morphology of the deposited copper. Absence of CRV, leads to three-dimensional with the formation of copper crystallites and in presence of crystal violet the growth of crystallites are perpendicular to the surface was reduced. Also, Carlos et al [22] found that CRV was essential to measure a significant response to glucose.

Apart from this crystal violet modified GCE [23], interaction of heparin with crystal violet and its applications [24], spectrophotometric and voltammetric interaction of heparin with CV and its analytical applications [25] and electrocatalytic oxidation of hydroquinone at poly(crystal-violet) film-modified electrode and its selective determination in the presence of o-hydroquinone and m-hydroquinone also reported [26]. Various types of electrochemical analysis have been reported for the detection and determination of arsenic [27]. Comparing with analytical techniques, modified electrodes keen special attention for the detection and determination of important chemical compounds due its easy preparation method, compatibility, reliability and wide electroanalytical applications [28-39]. For example, arsenic oxidation at platinum electrode [40], detection and determination of copper and arsenic by stripping voltammetry [41] and poly (3, 4-ethylenedioxythiophene) (PEDOT) film modified electrode to monitor iodide and arsenic sensing were reported [42]. These reports clearly show the

importance and the pathway for the arsenic detection using electrochemical methods. Therefore, in this report, we have attempted to fabricate a simple, rapid and reliable film for the sensitive detection and determination of arsenic at the micro levels in both the lab and real samples. Nano Au-CRV film has been fabricated on GCE and ITO by using cyclic voltammetry (CV). Surface morphological studies of the proposed film have been analyzed using field emission scanning electron microscopy (FE-SEM). The nano Au-CRV film modified GCE showed significant response for the detection of arsenic in lab and real samples using differential pulse voltammetry and impedimetric analysis.

## 2. EXPERIMENTAL

### 2.1. Apparatus

Electrochemical measurements like cyclic voltammetry (CV) and differential pulse voltammetry (DPV) was performed using CHI 1205A and 750A analyzers. A conventional three-electrode cell were used at room temperature with glassy carbon electrode (GCE) (surface area = 0.07 cm<sup>2</sup>) as the working electrode, Ag/AgCl (saturated KCl) electrode as reference electrode and a platinum wire as counter electrode.

The potentials mentioned in all experimental results were referred to standard Ag/AgCl (saturated KCl) reference electrode. Surface morphology of the film was studied by FE-SEM (Hitachi, Japan). Indium tin oxide (ITO) thin film coated glass electrodes have been used for the SEM analysis. Electrochemical impedance studies (EIS) were performed by using ZAHNER impedance analyzer (ZAHNER Elektrik GmbH & Co KG, Germany).

### 2.2. Reagents

Potassium tetra chloro Aurate (III) was purchased from Stem chemicals (USA) and Crystal violet (CRV) and sodium meta arsenite were purchased from Sigma – Aldrich (USA). The other chemicals (Merck) that are used in this investigation were of analytical grade (99 %). All the solutions are prepared using double distilled water.

Electrocatalytic studies were carried out in phosphate buffer solution (PBS) of pH 7.0 was prepared from Na<sub>2</sub>HPO<sub>4</sub> (0.05 M) and NaH<sub>2</sub>PO<sub>4</sub> (0.05 M). Pure nitrogen gas was passed through all solutions. Xindian river water (Taiwan (R.O.C)) obtained for the river water analysis. River water has been filtered several times before the analysis. Tap water was obtained from Taipei Water Department ([www.twd.gov.tw](http://www.twd.gov.tw)).

Tap water has been filtered several before the analysis. Two types of natural drinking spring water bottles obtained from local convenient store. Drinking spring waters directly employed without any further pretreatment process. Drinking spring water sample (1) contains, ((Ca<sup>+</sup>) 8–20, (Mg<sup>+</sup>) 2–6, (Na<sup>+</sup>) 6–15, (K<sup>+</sup>) 0.3–2 and (SiO<sub>2</sub>) 23–35 ppm; pH: 6.5–8.5). Drinking spring water type (2) contains Ca = 14.8 – 27.6, Mg = 8.8 – 16.4, Fe < 0.018, F < 0.1, and Na = 2.7 – 11.3 mg/L; pH 6.0–8.0. As (III)

was dissolved in this samples and the stock solution have been prepared and these solutions directly injected in the pH 7.0 PBS for the analysis.

### 2.3. Fabrication of nano Au-CRV film

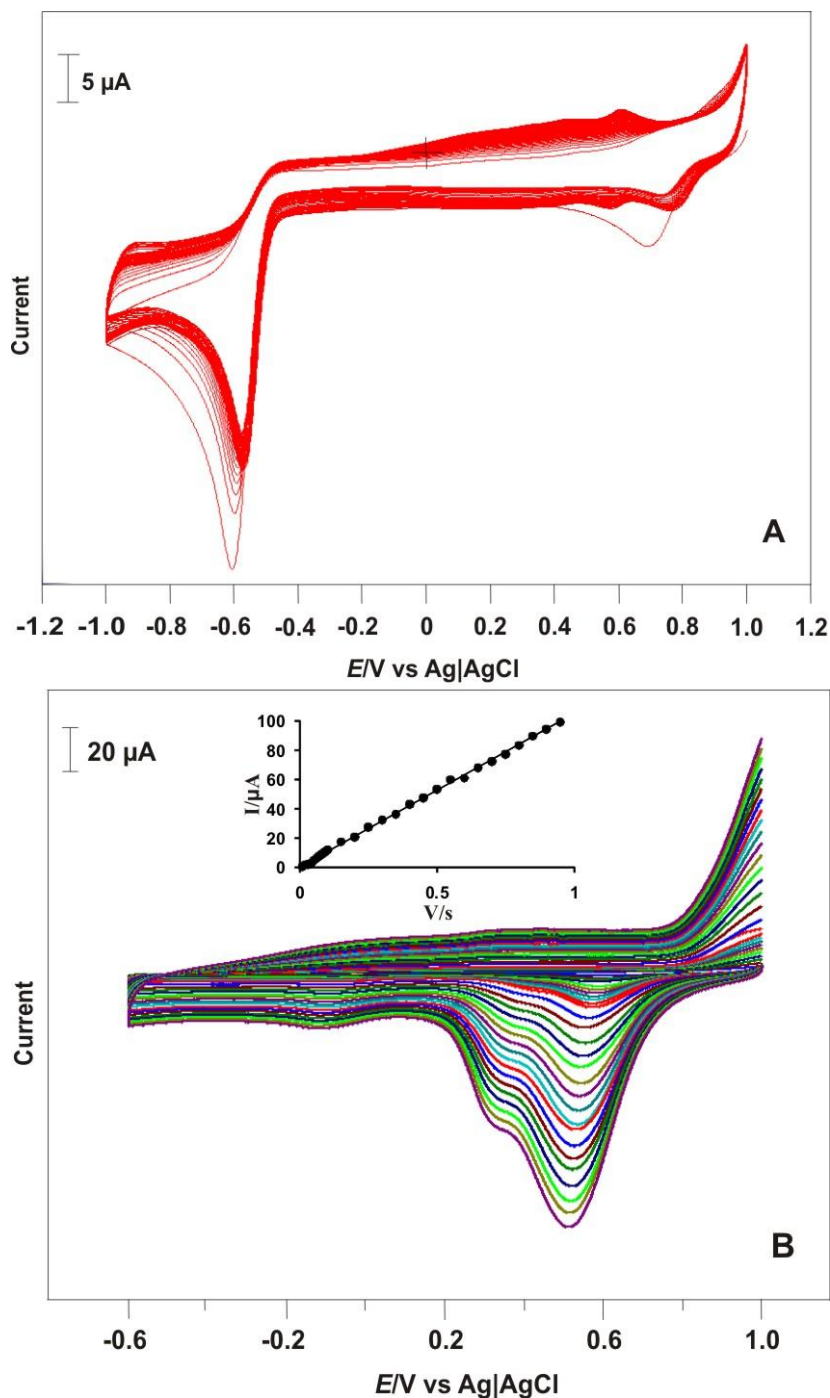


**Figure 1.** (A) CVs of nano Au-CRV film electrodeposited on the GCE from 0.1 M  $\text{KNO}_3$  containing  $\text{KAuCl}_4 \cdot 3\text{H}_2\text{O}$  ( $1 \times 10^{-3}$  M) and CRV ( $1 \times 10^{-3}$  M) and potential scan between 1 to -1 V for 60 cycles at the scan rate of 0.1 V/s. (B) Different scan studies of the nano Au-CRV film modified GCE in pH 7 PBS at the scan rate of 0.01-1 V/s. Inset shows the plot of Au reduction current vs. scan rate.

The bare GCE was initially polished with 0.05 $\mu\text{m}$  alumina powder on BAS polishing pad and ultrasonically cleaned in water for a minute. The electrode was then successfully washed with double distilled water and used. The GCE was modified by electrochemical deposition of gold nanoparticles ( $10^{-3}$  M) and crystal violet (CRV) ( $10^{-3}$  M) in 0.1 M  $\text{KNO}_3$  solution in the potential scan between 1 and -1 V, at the scan rate of 0.1  $\text{V s}^{-1}$  for sixty cycles (Figure 1(A)). Finally, the nano Au-CRV film modified GCE was then rinsed with double distilled water and used for further electrochemical studies.

### 3. RESULTS AND DISCUSSION

#### 3.1. Characterization of nano Au-CRV film

Figure 1(A) displays the electrochemical deposition process of nano Au-CRV film which begins at the positive potential of 1.0 V and ends in the negative potential -1 V at the scan rate of 0.1 V/s for sixty cycles. Here the reduction of Au takes place at the potential of 0.75 V and continues up to -1 V and at the higher reduction peak current occurred at the -0.6 V in the first scan process. This result clearly shows the initial nucleation of Au at the electrochemical deposition process. For the continuous cycles, this peak current decreases with the potential shift and initiates at -0.58 V. During the electrochemical deposition process, the continuous growth of the reduction and oxidation peak currents of Au validates the electrochemical deposition process of nano Au-CRV film on the GCE surface. To verify the CRV deposition process, only CRV film has been electrodeposited on the GCE (Fig not shown). In the only CRV deposition process, there is a sharp increase in the anodic peak currents (1 V) and at the cathodic peak currents (-1 V) and no any specific redox peaks found for the CRV electrochemical deposition process. Based on this result, we conclude that the electrochemical deposition of CRV occurs with the nano Au deposition process and it exhibits as a thin layer on the electrode surface.

Next the nano Au-CRV film modified GCE was employed for the different scan rate studies in pH 7.0 PBS. Figure 1(B) displays the different scan rate studies of the nano Au-CRV film at the scan rate of 0.01-1 V/s. For the increasing scan rates, the reduction peak current of Au increases and shifts to negative potentials. Further this peak currents were linearly dependent on the scan rate illustrates that the nano Au-CRV film possesses the surface controlled electrochemical activity. The linear regression equation for the Au peak current was expressed as  $I_{\text{pc}} (\mu\text{A}) = 104.6v (\text{V/s}) + 0.0527$ ,  $R^2 = 0.999$ .

#### 3.2. Impedimetric and SEM analysis

Nano Au-CRV film has been examined using electrochemical impedance analysis. Electrochemical impedance analysis is generally studied by utilizing an equivalent circuit model, which suites and associates with the electrochemical properties of the film modified GCE. Nyquist plot of electrochemical impedance spectra generally explicates the electron transfer nature of the film. Figure 2 displays the Nyquist plots of the bare (curve a) and nano Au-CRV film (curve b) modified

GCEs in pH 7 PBS containing 5 mM  $[\text{Fe}(\text{CN})_6]^{3-/4-}$ . The respective semicircle parameters correspond to the electron transfer resistance ( $R_{\text{et}}$ ) and the double layer capacity ( $C_{\text{dl}}$ ) of the film. As can be seen in Figure 2, bare GCE exhibits a semi circle area ( $R_{\text{et}} = 1050 \Omega$ ) which is larger than the nano Au-CRV film ( $R_{\text{et}} = 570 \Omega$ ). This result illustrates that the nano Au-CRV film possesses the lower electron transfer resistance comparing with the bare GCE which enhances the electron-transfer kinetics process as a faster one and more suitable for the electrocatalytic activities.

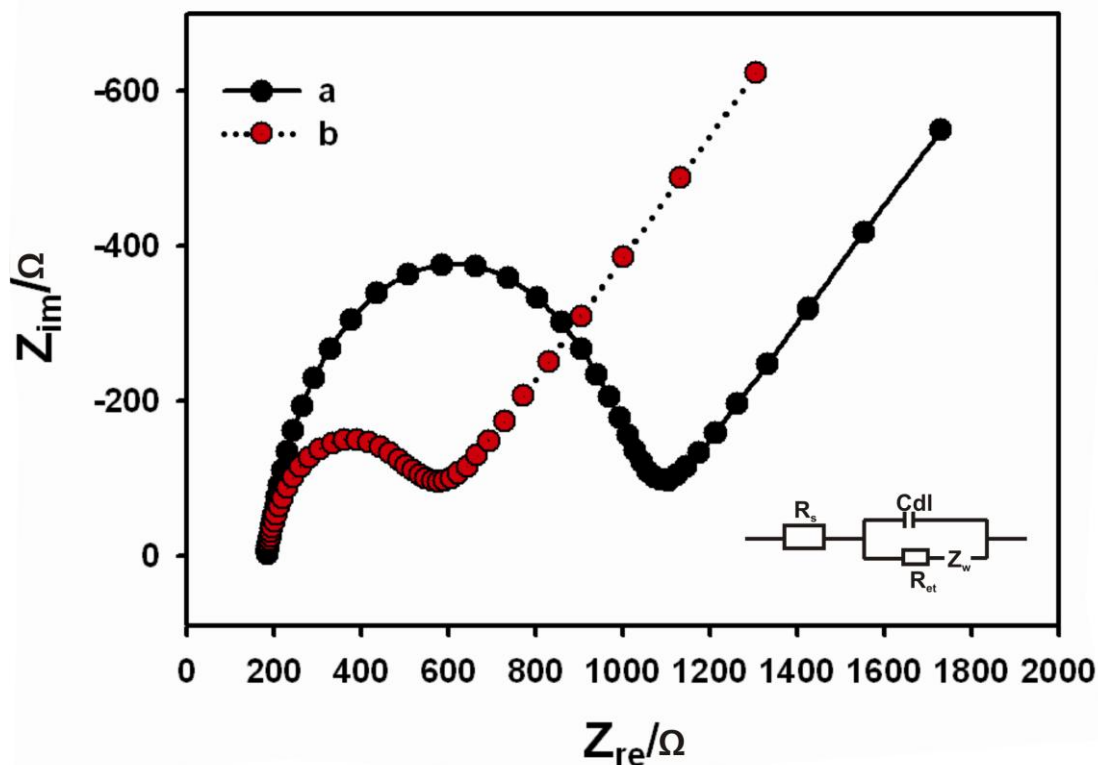


**Figure 2.** EIS response of (a) bare and (b) nano Au-CRV film modified GCE in pH 7 PBS containing 5 mM  $[\text{Fe}(\text{CN})_6]^{3-/4-}$ . Inset shows the simple Randles circuit model for the nano Au-CRV film.

A simplified Randles circuit model (Fig 2(inset)) has been used to fit the impedance spectra. The Randles circuit model well suits with the impedance spectroscopic results and the fit model error for the film was found as 7.3 %. Finally the electrochemical impedance spectroscopic analysis clearly illustrates the electrochemical behavior of the nano Au-CRV film.

Next the nano Au-CRV film modified ITO has been employed for the FE-SEM analysis. Figure 3(A) and (B) shows the large scale view [ $\times 10,000$  ( $1 \mu\text{m}$ )] and magnified views [ $\times 40,000$  ( $100 \text{ nm}$ )] of electrodeposited Nano Au-CRV film modified ITO. Based on Fig. 3(A) and (B) we can clearly see the existence of electrodeposited nano Au particles on the ITO surface. CRV has been co-deposited as thin film on the ITO surface. However the co-electrodeposited CRV not distinguishable one in the FE-SEM analysis because it has been deposited as a very thin layer on the electrode surface. Here the electrodeposited nano Au particles sizes were found in the range of 20-80 nm. During the

electrodeposition process, few nano Au particles coagulated together and deposited as group of nanoparticles. These nanoparticles size falls in the range of 100-150 nm. Finally, FE-SEM results clearly explicate the surface morphological nature of the nano Au-CRV film.

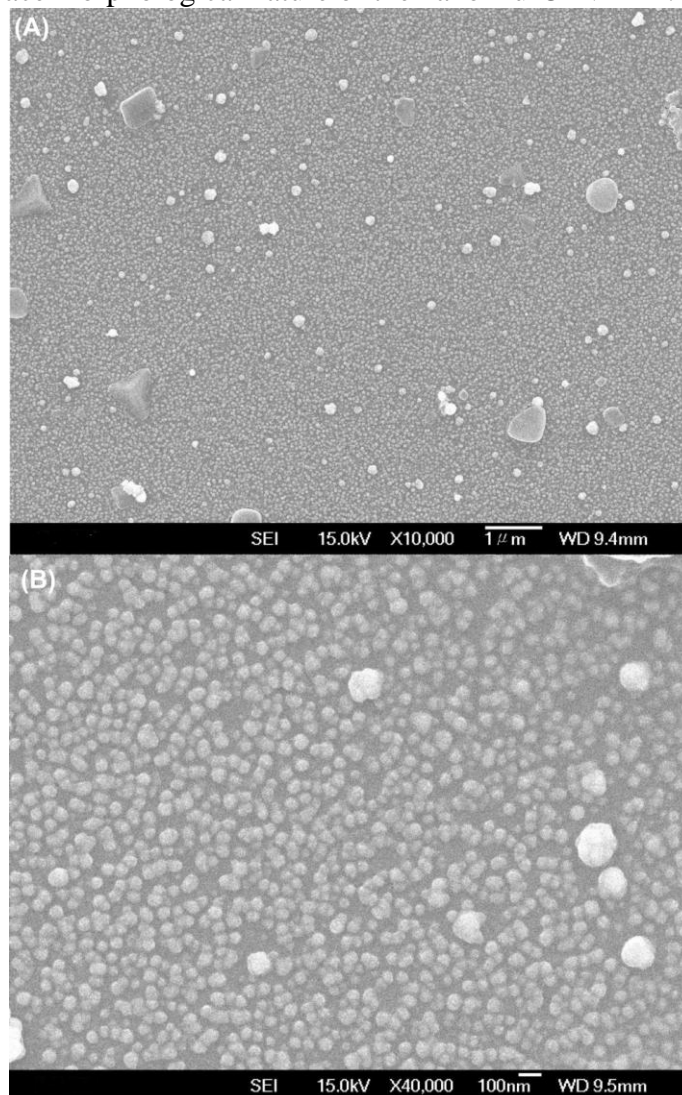


**Figure 3.** SEM images of the nano Au-CRV film modified ITO (magnifications x10, 000 (A) and x40,000 (B)).

### 3.3. Electrochemical detection of arsenic

Electrochemical detection of As (III) has been examined by CV (Figure 4(A)). Figure 4(A) curve (b) shows the detection of As (III) ( $4 \times 10^{-5}$  M) at nano Au-CRV film modified GCE. The As (III) electrochemical detection signal appears at 0.5 V on the nano Au-CRV film modified GCE in pH 7.0 PBS. At the same time, the CRV film modified GCE (curve c) not showed obvious response for the detection of As (III). Bare GCE (curve a') also showed the null response for the detection of As (III) detection. The above result clearly shows that the nano Au-CRV film modified GCE shows excellent response for the detection of As (III) in pH 7.0 PBS. Based on this examination further we have employed the nano Au-CRV film modified GCE for the detailed detection of As (III) using DPV.

Figure 4(B) (curve a-t), show the DPVs of nano Au-CRV film modified GCE in pH 7.0 PBS for the various concentrations of As (III). Here the electrochemical detection signal of As (III) appears at 0.47 V. Nano Au-CRV film modified GCE also exhibits a small oxidation peak current for As (III) detection at around -0.07 V.

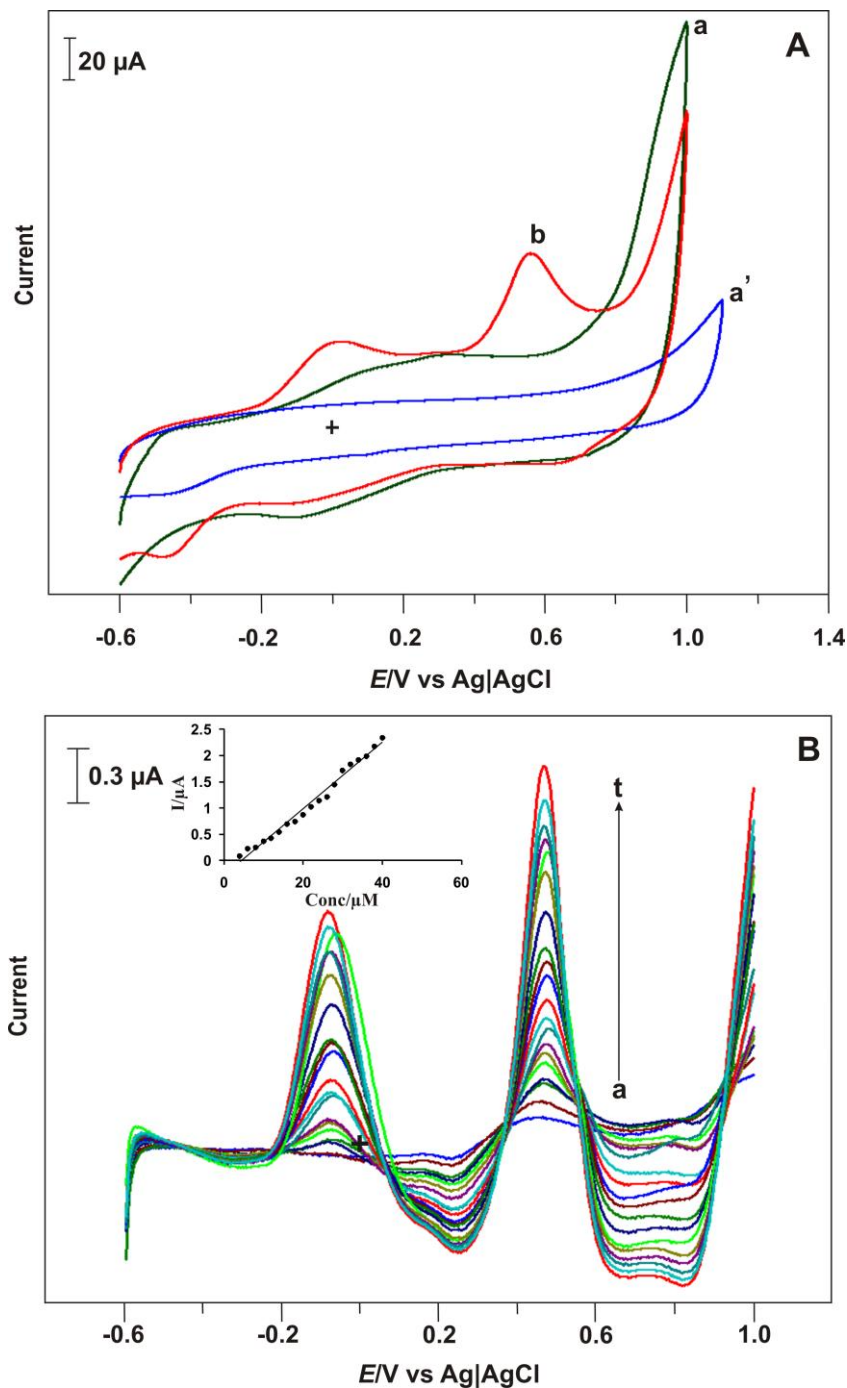


**Figure 4.** (A) (a) Nano Au-CRV film modified GCE in pH 7 PBS, (b) electrocatalytic response of (b) nano Au-CRV film and (c) only CRV film modified GCE for As (III) detection ( $4 \times 10^{-5}$  M). (a') Bare GCE response for As (III) ( $4 \times 10^{-5}$  M). (B) DPVs of nano Au-CRV film modified GCE for the different concentrations of As (III) (lab sample) in pH 7 (a-t; 2, 4, 6, 8, 10, 12, 14, 16, 18, 20, 22, 24, 26, 28, 30, 32, 34, 36, 38, 40  $\mu$ M) Inset shows calibration plot of As (III) detection.

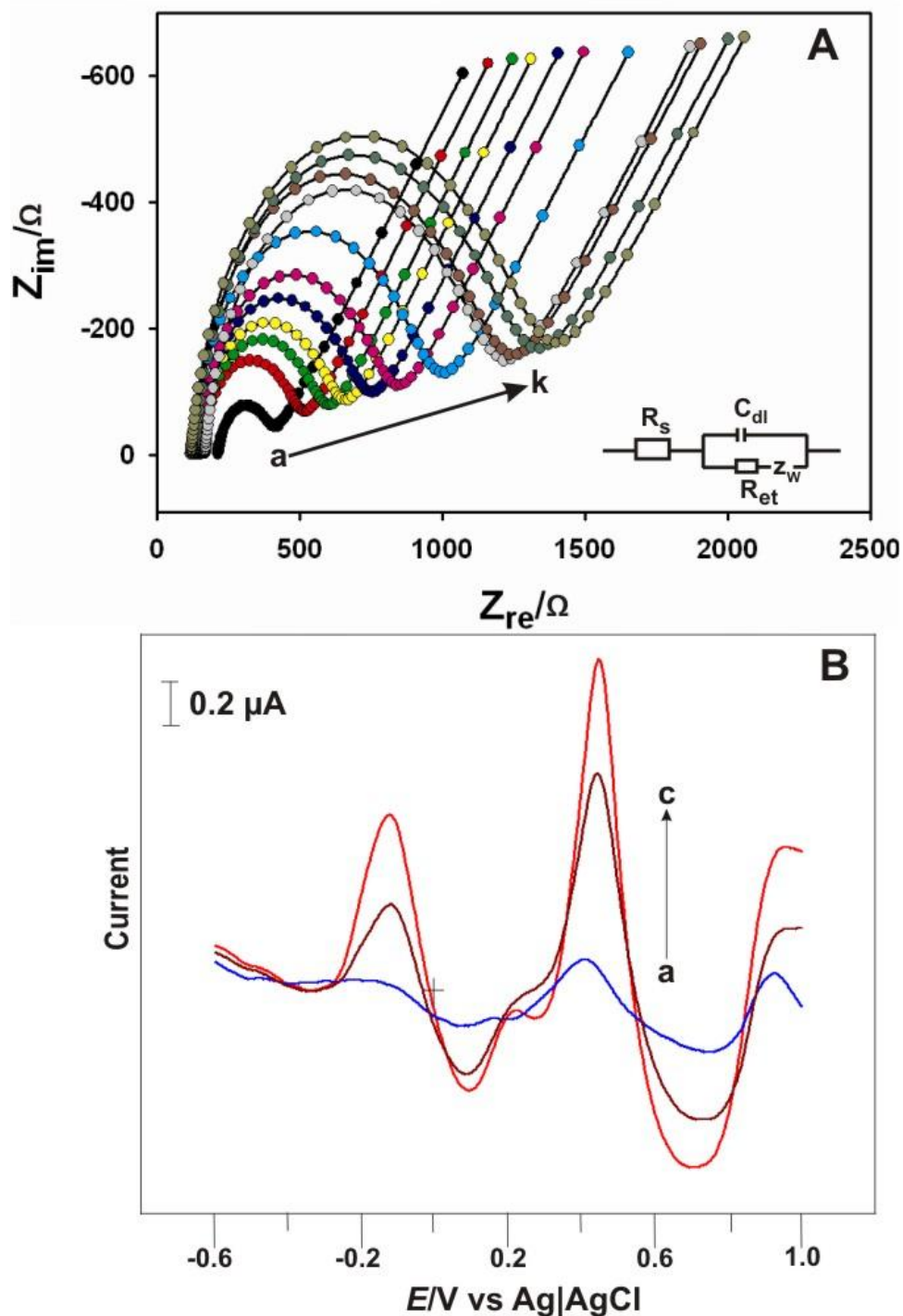


**Figure 5.** (A) EIS response of nano Au-CRV film modified GCE for the various concentrations of As (III) in pH 7 PBS containing 5 mM  $[\text{Fe}(\text{CN})_6]^{3-/4-}$ . As (III) concentrations were (a-k): 2, 4, 6, 8, 10, 12, 14, 16, 18, 20, and 22  $\mu\text{M}$ . Inset shows Inset shows the randles circuit of the above figure. (B) DPVs of nano Au-CRV film modified GCE for the As(III) detection (a) As (III) (2  $\mu\text{M}$ ), (b) As (III) (12  $\mu\text{M}$ ) +  $\text{CuSO}_{4.5}\text{H}_2\text{O}$  (4  $\mu\text{M}$ ) and (c) As (III) (20  $\mu\text{M}$ ) +  $\text{Pb}(\text{NO}_3)_2$  (2  $\mu\text{M}$ ).

For the continuous additions of As (III), the nano Au-CRV film shows well distinguished anodic oxidation peaks which linearly dependent on the increasing concentrations of As (III), respectively. This result validates the capability of the proposed film will be suitable for the detection

of As (III) in the certain linear ranges (2-40  $\mu\text{M}$ ) in pH 7.0 PBS. The inset of Figure 4(B) shows the current versus calibration plot for the As (III) detection. The sensitivity and the detection limit of the As (III) detection at the nano Au-CRV film modified GCE was found as  $0.8075 \mu\text{A } \mu\text{M}^{-1}\text{cm}^2$  and 0.20  $\mu\text{M}$ . The relative standard deviation (RSD) of the As (III) determination (40  $\mu\text{M}$ ) for the ten repeated measurements at the same nano Au-CRV film modified GCE was found as 6.42 % which shows the virtuous repeatability nature of the proposed film. Furthermore, the reproducibility of the film has been examined using four individual GCEs modified with the proposed film and for the fixed concentration of As (III) (40  $\mu\text{M}$ ) the RSD was found as 2.23 %, respectively.

### 3.4. Impedimetric detection and interference studies

Electrochemical impedance spectroscopy is another alternative technique for the impedimetric detection of important compounds using the film modified electrodes. Figure 5(A) show the Nyquist curves obtained for the electrochemical detection of As (III) at the nano Au-CRV film modified GCE. Open circuit potential has been applied for the impedimetric detection process. As (III) was added in the concentration rang of 2-22  $\mu\text{M}$ . The electron transfer resistance ( $R_{\text{et}}$ ) of nano Au-CRV film were clearly increases which is concordant with the increasing concentrations of As (III) in pH 7.0 PBS containing 5 mM  $[\text{Fe}(\text{CN})_6]^{3-/4-}$ . Here the  $R_{\text{et}}$  clearly increase with the increasing concentration of As (III), which gives rise to a linear-type detection response from 2-22  $\mu\text{M}$ . This is because the adsorption of As (III) on the film surface which further hinders the electron-transfer kinetics at the film surface. Moreover, the detection response falls up to 22  $\mu\text{M}$ , which indicates the film's saturation limit for the adsorption of As (III).

In the next step interference studies have been carried out for the As (III) detection process. In the industrial waste water analysis copper and lead found to be major interfering compounds in the detection of As (III). Hence the electrochemical detection of As (III) has been examined with these interfering compounds. Figure 5(B) shows the interference studies at the nano Au-CRV film modified GCE for the detection of As (III). For the mixture of additions of As (III) with  $\text{CuSO}_4$ , and  $\text{Pb}(\text{NO}_3)_2$  the proposed film obviously shows the anodic oxidation signals of As (III) apparently. This result validates that the nano Au-CRV film overcomes the interference signals and successfully shows the As (III) detection signals in pH 7.0 PBS.

### 3.5. Arsenic detection in various water samples

The real sample analysis has been carried out using real world drinking water sources like river water (Xindian River, Taipei, Taiwan (ROC), spring waters (sample 1 and sample 2) and tap water (Taipei water department, Taiwan (ROC)). As (III) dissolved river water has been spiked in pH 7.0 PBS (Figure 6(A)). The nano Au-CRV film modified GCE clearly exhibits the As (III) detection signals (at 0.51 V) in the linear range of 2-72  $\mu\text{M}$ . The sensitivity and detection limit of the nano Au-CRV film for the As (III) detection was found as  $0.686 \mu\text{A } \mu\text{M}^{-1}\text{cm}^2$  and 0.28  $\mu\text{M}$ . The above result shows that the proposed film holds the capability to detect the As (III) in river water.

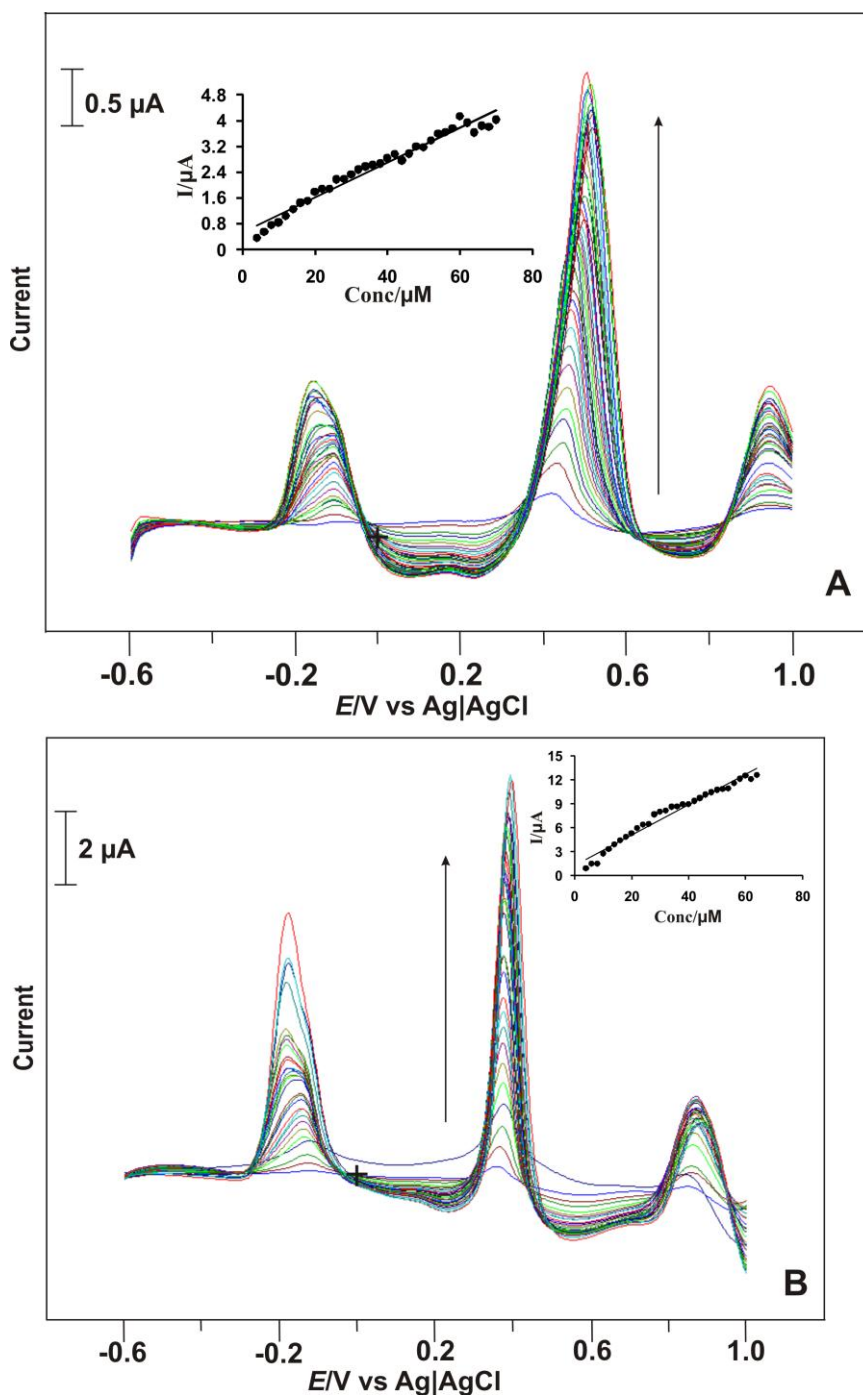


**Figure 6.** (A) DPVs of nano Au-CRV film modified GCE for As (III) detection (dissolved in river water) in pH 7 PBS (As (III) concentration: 2, 4, 6, 8, 10, 12, 14, 16, 18, 20, 22, 24, 26, 28, 30, 32, 34, 36, 38, 40, 42, 44, 46, 48, 50, 52, 54, 56, 58, 60, 62, 64, 66, 68, 70, 72 μM). Inset shows calibration plot of As (III) detection in river water. (B) DPVs of nano Au-CRV film modified GCE for As (III) (dissolved in spring water-1) in pH 7 PBS (As (III) concentration: 2, 4, 6, 8, 10, 12, 14, 16, 18, 20, 22, 24, 26, 28, 30, 32, 34, 36, 38, 40, 42, 44, 46, 48, 50, 52, 54, 56, 58, 60, 62, 64 μM). Inset shows calibration plot of As (III) in drinking mineral water (A).

Next the drinking spring water samples (sample-1(Figure-6(B)) and sample-2 (Figure-7(A)) (mineral content details has been included in the experimental section)) have been employed for the

detection of As (III). In the spring water sample-1 the linear range of detection of As (III) was found as 2 to 64  $\mu\text{M}$ . The sensitivity and the detection limit of the nano Au-CRV film for As (III) detection in the sample-1 was found as  $2.41 \mu\text{A} \mu\text{M}^{-1}\text{cm}^2$  and  $0.69 \mu\text{M}$ .

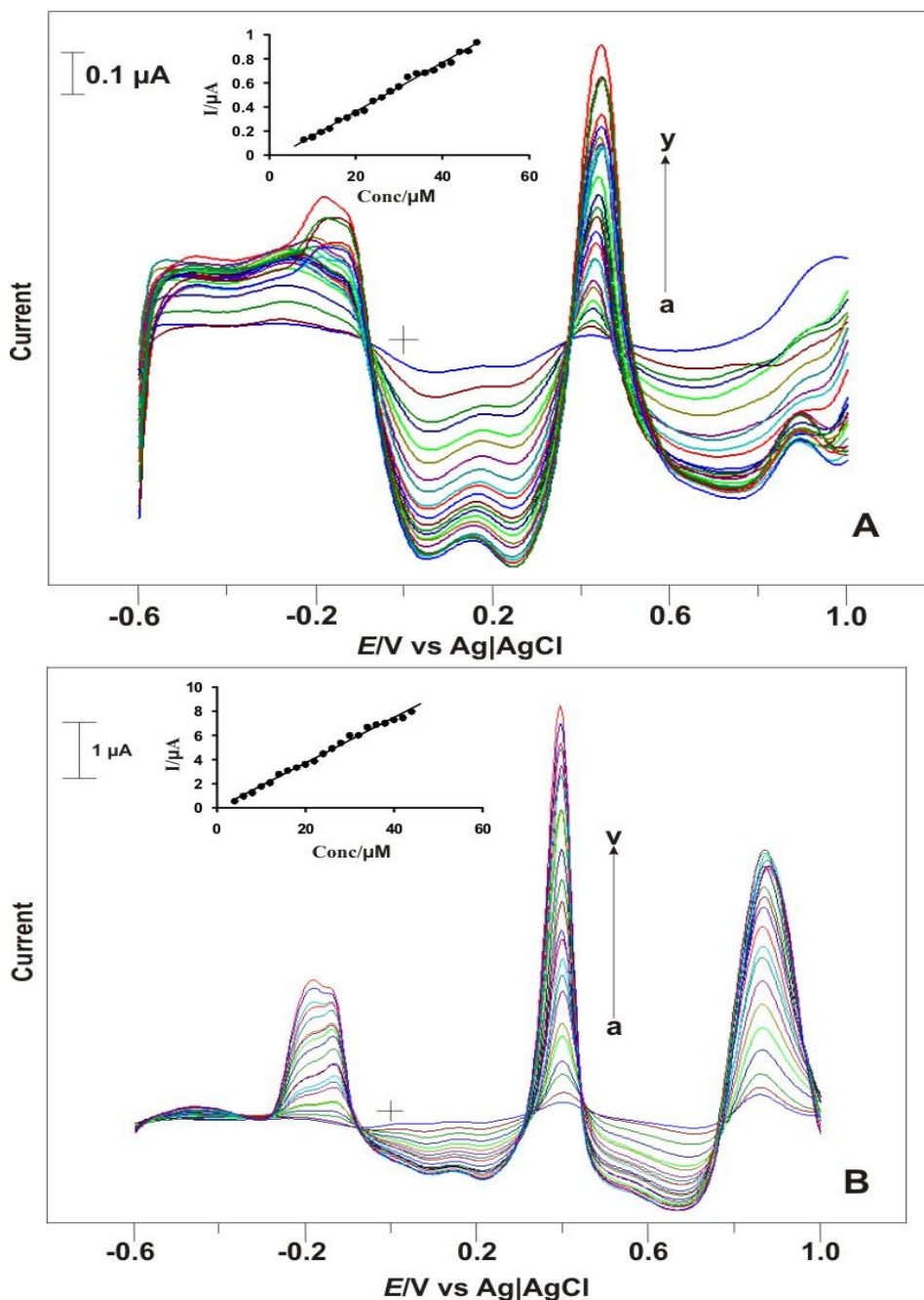


**Figure 7.** (A) DPVs of nano Au-CRV film modified GCE for As (III) detection (dissolved in spring water-2) in pH 7 PBS (As (III) concentration (a-y): 2, 4, 6, 8, 10, 12, 14, 16, 18, 20, 22, 24, 26, 28, 30, 32, 34, 36, 38, 40, 42, 44, 46, 48, 50  $\mu\text{M}$ ). Inset shows calibration plot of As (III) in drinking mineral water. (B) DPVs of nano Au-CRV film modified GCE for As (III) detection (dissolved in tap water) in pH 7 PBS (As (III) concentration (a-v): 2, 4, 6, 8, 10, 12, 14, 16, 18, 20, 22, 24, 26, 28, 30, 32, 34, 36, 38, 40, 42, 44, 46, 48  $\mu\text{M}$ ). Inset shows calibration plot of As (III) in tap water.

Next, in the sample-2 nano Au-CRV film modified GCE detects the As (III) in the linear range of 2 to 50  $\mu\text{M}$  with the sensitivity and detection limit of  $0.256 \mu\text{A} \mu\text{M}^{-1}\text{cm}^2$  and  $0.76 \mu\text{M}$ . These two results clearly explicates that the proposed film successfully detects the As (III) in the drinking spring water samples, respectively.

Finally tap water has been examined for the As (III) detection process (Figure 7(B)). As (III) dissolved tap water was spiked in pH 7.0 PBS and the nano Au-CRV film modified GCE clearly shows the electrochemical detection signals of As (III) (at 0.39 V) in the linear range of 2-48  $\mu\text{M}$ . Sensitivity and the detection limit of the proposed film for the As (III) detection was  $2.38 \mu\text{A} \mu\text{M}^{-1}\text{cm}^2$  and  $0.36 \mu\text{M}$ . Sensitivity and the detection limit of the nano Au-CRV film for As (III) detection in this analysis may vary due to the different types of the real samples. Finally, all these water sample analysis results clearly show that the proposed film possesses the capability to detect the As (III) successfully in the real samples.

#### 4. CONCLUSION

Electrochemically fabricated nano Au-CRV film modified GCE successfully employed for the detection of As (III) using CV and DPV. The proposed film overcomes the interference effects and shows only the As (III) detection signals at the stipulated conditions. The nano Au-CRV film successfully employed for the detection of As (III) in the micro molar concentration ranges in the real drinking water samples such like, river water, spring water and tap water samples. The proposed film will be a promising method for the detection of As (III) in electroanalysis and this method could be utilized for the detection of As (III) in the lab and real samples along with verification of other analytical techniques.

#### ACKNOWLEDGMENT

This work was supported by grants from National Science Council (NSC) of Taiwan (ROC).

#### References

1. C.M. Su and M. Androbert, *Environ. Sci. Technol.*, 1487 (2001) 35.
2. B. K. Mandal and K.T. Suzuki, *Talanta*, 201 (2002) 58.
3. World Health Organization, website: [www.who.int/entity/watersanitation/health/dwq/arsenicun8.pdf](http://www.who.int/entity/watersanitation/health/dwq/arsenicun8.pdf).
4. World Health Organization, website: [www.who.int/mediacentre/factsheets/fs210/en/](http://www.who.int/mediacentre/factsheets/fs210/en/).
5. C. Wei and J. Liu, *Talanta*, 540 (2007) 73.
6. World Health Organization, website: [www.who.int/entity/water\\_sanitation/health/dwq/arsenicun2.pdf](http://www.who.int/entity/water_sanitation/health/dwq/arsenicun2.pdf).
7. N. Campillo, R. Peñalver, P. Viñas, I. L.García and M. H. Córdoba, *Talanta*, 793 (2008) 77.
8. P. Salaün, B. P.Friedrich and C. M.G. Van den Berg, *Anal. Chim. Acta*, 312 (2007) 585.
9. X. Dai, O. Nekrassova, M.E. Hyde, and R. G. Compton, *Anal. Chem.*, 5924 (2004) 76.
10. E. Majid, S. Hrapovic, Y. Liu, K. B. Male and J. H. T. Luong, *Anal. Chem.*, 762 (2006) 78.

11. X. Dai and R. G. Compton, *Analyst*, 516 (2006) 131.
12. L. Xiao, G. G. Wildgoose and R. G. Compton, *Anal. Chim. Acta*, 44 (2008) 620.
13. J. Vandenheck, M. Waeles, R. D. Riso and P. L. Corre, *Anal. Bioanal. Chem.*, 929 (2007) 388.
14. L. Rassaei, M. Sillanp, R.W. French, R.G. Compton and F. Markenc, *Electroanalysis*, 1286 (2008) 20.
15. S. Hrapovic, Y. Liu and J. H. T. Luong, *Anal. Chem.*, 500 (2007) 79.
16. B.K. Jena and C.R. Raj, *Anal. Chem.*, 4836 (2008) 80.
17. S. C. Mathur, G. D. Sharma, D. C. Dube, *Thin Solid Films*, 249 (1988) 164.
18. P. Vanysek, I.C. Hernandez, J.J. Xu, *J. Colloid Interf Sci.*, 527 (1990) 139.
19. T. Stanoeva, D. Neshchadin, G. Gescheidt, J. Ludvik, B. Lajoie, S.N. Batchelor, *J. Phys. Chem A* 11103 (2005) 109.
20. A.S. Dakkouri, N. Batina and D. M. Kolb, *Electrochim. Acta* 2467 (1993) 38.
21. W. Haiss, D. Lackey and J.K. Sass, *Chem. Phys.lett.*, 343 (1992) 200.
22. C.P. Ramirez and D. J. Caruana, *Electrochem. Commun.*, 450 (2006) 8.
23. V.V. Perekotii, Z.A. Temerdashev, T.G. Tsyupko, and E.A. Palenaya, *J. Anal. Chem.*, 448 (2002) 57.
24. W. Sun, Y. Ding, and K. Jiao, *J. Anal. Chem.*, 359 (2006) 61.
25. W. Sun, J.-Y. Han, Q.-J. Li and K. Jiao, *S. Afr. J. Chem.*, 42 (2007) 60.
26. Y. Zhang, H.S. Zhuang, and H. Lu, *Anal. Lett.*, 339 (2009) 42.
27. C. Ruíz, J. M. Anaya, V. Ramírez, G. I. Alba, M. G. García, A. Carrillo-Chávez, M. M. Teutli, E. Bustos, *Int. J. Electrochem. Sci.*, 6 (2011) 548.
28. S.-M. Chen S.-H. Li, S. Thiagarajan, *J. Electrochem. Soc.*, 154 (2007) E123.
29. M. M. Ardakani, Z. Taleat, *Int. J. Electrochem. Sci.*, 4 (2009) 694.
30. S. Thiagarajan, S.-M. Chen, K.-H. Lin, *J. Electrochem. Soc.*, 155 (2008) E33.
31. B.-W. Su, S. Thiagarajan, S.-M. Chen, *Electroanalysis* 20 (2008) 1987.
32. H. R. Zare, R. Samimi, M. M. Ardakani, *Int. J. Electrochem. Sci.*, 4 (2009) 730.
33. G. Guo, F. Zhao, F. Xiao, B. Zeng, *Int. J. Electrochem. Sci.*, 4 (2009) 1365.
34. T.-H. Tsai, S. Thiagarajan, S.-M. Chen, *J Appl. Electrochem.*, 40 (2010) 2071.
35. C.-Y. Cheng, S. Thiagarajan, S.-M. Chen, *Int. J. Electrochem. Sci.*, 6 (2011) 1331.
36. M. Rajkumar, S. Thiagarajan, S.-M. Chen, *J. Appl. Electrochem.*, 41 (2011) 663.
37. T.-H. Tsai, S.-H. Wang, S.-M. Chen, *Int. J. Electrochem. Sci.*, 6 (2011) 1655.
38. S. Thiagarajan, C.-Y. Cheng, S.-M. Chen, T.-H. Tsai, *J. Solid. Electrochem.*, 15 (2011) 781.
39. S. Thiagarajan, T.-H. Tsai, S.-M. Chen, *Int. J. Electrochem. Sci.*, 6 (2011) 2235.
40. P. Shakkthivel, P. Singh, *Int. J. Electrochem. Sci.*, 2 (2007) 311.
41. F. R. Bento, M. T. Grassi, A. Sales, L. H. Mascaro, *Int. J. Electrochem. Sci.*, 3 (2008) 1523.
42. T.-W. Chen, T.-H. Tsai, S.-M. Chen, K.-C. Lin, *Int. J. Electrochem. Sci.*, 6 (2011) 2043.